CrystEngComm

Accepted Manuscript

The Polymorphism of a Triarylphosphine oxide. A case of missing isomers.

Cristina Puigjaner,*[a] Sergi Vela,[b] Mercè Font-Bardia,[c] and Juan J. Novoa*[b]

[a] *Unitat de Polimorfisme i Calorimetria, Centres Cientificotècnics, Universitat de Barcelona, Baldiri Reixac, 10, 08028 Barcelona, Spain. Fax: 34 934037206; Tel: 34 934034656; E-mail: cris@ccit.ub.edu*

[b] *Departament de Química Física & IQTCUB, Facultat de Química, Universitat de Barcelona, Martí i Franquès 1, 08028, Barcelona, Spain; E-mail: juan.novoa@ub.edu*

[c] *Unitat de Difracció de Raigs X, Centres Cientificotècnics, Universitat de Barcelona, Lluís Solé i Sabarís, 1-3, 08028 Barcelona, Spain.*

ABSTRACT

An experimental and computational study of the polymorphism of *o*-nitrophenyldiphenylphosphine oxide (**1**) has been carried out. Two polymorphs of **1** have been obtained after a comprehensive screening procedure and their structure has been determined by single crystal diffraction. Both forms present the same racemic mixture of the *Ps* and *Ms* enantiomers, where the NO_2 is in a *syn* conformation relative to the PO group, thus resulting in the presence of a short $PO\cdots O_2N$ contact (of *ca.* 2.97Å). The *anti* conformation has not been found in any of these polymorphs, thus suggesting the attractive nature of the $PO\cdots O_2N$ intramolecular interaction. However, MP2 computations on various model systems led to the conclusion that this interaction is energetically destabilizing. An energy analysis of all the symmetry-unique pairs found within the first-nearest neighbour of the experimental polymorphs (all with a *syn* conformation), and of their corresponding (non-observed) *anti* conformations, reveals a slightly higher stability of the former. Therefore, if the crystallizations of both polymorphs of **1** were only dominated by the energetics of this molecule, the *syn* and *anti* conformations should both be present in the crystals. The absence of the latter suggests that the final outcome of these crystallizations is not solely determined by the **1**···**1** intermolecular interactions. Instead, **1**-solvent interactions, the presence of nucleation-driving centres, for instance, in the container-solution interface, and kinetic factors of the nucleation process, could also be relevant or play a leading role.

INTRODUCTION

Triarylphosphine oxides (Ar_3PO), also known as molecular propellers, are a class of compounds composed of three aryl groups arranged in a helical fashion about a central atom. Ar_3PO compounds are valuable reagents, additives or ligands in synthetic chemistry[1] and some substituted Ar_3PO have also been used for inhibiting certain taste functions and perceptions in pharmaceuticals and food.[2] In 1988, M. C. Etter described the cocrystallization power of Ph_3PO for obtaining extraordinary beautiful crystals.[3] Moreover, these multiaryl systems exhibit interesting properties from the point of view of crystal engineering, originating from their torsional isomerism.[4] Changes in their *ortho*-substituents can profoundly influence the intramolecular geometry, thus affecting stability of the intermolecular arrangements and the crystal packing.

For a given *ortho*-substituent, we can find the relative stability of its two possible conformational isomers respect to the phosphorus atom (*syn* vs. *anti*).[5] Note that, each of these conformations may also exist as two enantiomeric forms, *P* (clockwise) or *M* (counterclockwise),[6] due to the fact that these tripodal compounds adopt a propellerlike C_3

conformation (fast inversion of helicity occurs at room temperature in solution[7]). Structures of the Ar_3PO type can be visualized as presenting four ligands (or pseudo-ligands) arranged in a quasi-tetrahedral fashion around a central P atom (Fig. 1). The three aryl carbons bonded to P define a plane called the *reference plane* (Fig. 1, in red). There are three ways any given aryl group may orient itself with respect to this plane: (1) the plane of the aromatic ring may be perpendicular to the reference plane, (2) the normal to the ring which passes through the carbon atom attached to P may lie in a plane perpendicular to the reference plane and containing the C-P bond, (3) or the plane of the aromatic ring may assume an intermediate position. Therefore, there are two unique conformations and an infinite number of intermediate conformations. All the Ar_3PO systems studied so far show one of the intermediate conformations.[8] All of this explains the continuing interest of substituted Ar_3PO molecules in crystal engineering. One of them is the object of our interest in this work: determining how *ortho*-substitutions in the aryl rings modify the packing of the resulting polymorphs (each experimental polymorph a local minimum in the free energy of the crystal[9]).
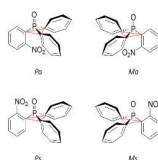
Fig. 1 Possible isomers *syn* (*Ps* and *Ms*) and *anti* (*Pa* and *Ma*) of *o*-nitrophenyldiphenylphosphine oxide (**1**)

Among the available Ar_3PO molecules whose polymorphism could be investigated, in this work we focus our attention in the polymorphism of *o*-nitrophenyldiphenylphosphine oxide (**1**). Molecules of **1** have two identical aryl groups (discarding central chirality) and one *ortho*-substituent attached to the remaining aryl group, which can be located in the two sides of the, above defined, reference plane (that may also be considered as a *plane of chirality*). The total number of possible isomers for **1** is equal to four: two *syn* and two *anti* isomers, each one having two directions of helicity *P* and *M* (thus resulting in the *Ps, Ms, Pa* and *Ma* isomers of Fig. 1). In this work we report the structural analysis of the two polymorphs of **1** obtained as result of a polymorphic screening. Both polymorphs show the same racemic mixture of *Ps* and *Ms* enantiomers of the *syn* conformation, the molecules of **1** showing a similar intramolecular disposition of their groups, where short $PO\cdots O_2N$ contacts (of *ca.* 2.97Å) are formed. Surprisingly, no *anti* isomers were isolated, thus suggesting the attractive nature of these $PO\cdots O_2N$ interactions. All these facts prompted us to determine, using accurate *ab initio* methods, the nature of the $PO\cdots O_2N$ interaction and to perform an energetic analysis of the structure of **1**, aimed at rationalizing why only the *syn* enantiomers (*Ps* and *Ms*) are found. Since a satisfactory answer was not achieved by looking at isolated molecules of **1**, we have also examined the crystal packing of one of the polymorphs. Specifically, we have computed the interaction energy of all symmetry-unique pairs of **1**, within the first-nearest neighbours, in the crystal structure of Form I (*d1-d6*). These energies will allow us to preclude the existence of structure-directing pairs (those having interaction energies notably larger than the others). In addition, the geometry of the (*d1-d6*) pairs has been allowed to optimize with each of their constituents being on the *syn* and *anti* conformations. By comparing their relative stability at their crystal and optimized structures, one can gain information on how the crystal packing determines the presence of, exclusively, the *syn* conformation in the known polymorphs of **1**.

EXPERIMENTAL SECTION

1. Synthesis of the polymorphic crystal forms

o-Nitrophenyldiphenylphosphine oxide **1** was synthesized from *o*-dinitrobenzene and ethyl diphenylphosphinite, as previously described:[10] ethyl diphenylphosphinite (2 g, 8.7 mmoles) was added in small portions to a solution of *o*-dinitrobenzene (1g, 5.9 mmoles) in dimethylformamide (3 mL) at -10ºC. On removal of the ice-bath, the mixture was stirred for 12 hours at room temperature. The precipitate that formed was filtered off, washed with dimethylformamide and recrystallised from ethanol (m.p. 224ºC).

Form I: crystallization of **1** from boiling ethylacetate yielded at room temperature pale yellow large plate crystals of several millimetres, suitable for X-ray diffraction.

Form II: crystallization of **1** from boiling toluene yielded at room temperature pale yellow block crystals suitable for X-ray diffraction.

A polymorphic screening was carried out with fourteen solvents, at several concentrations and temperatures, with variable cooling and evaporation rates, in both thermodynamic and kinetic conditions, yielding only Forms I and II.

2. Powder X-ray diffraction (PXRD)

Powder X-ray diffraction patterns were obtained on a PANalytical X'Pert PRO MPD diffractometer with a Cu Kα radiation (λ = 1.5418 Å) in a transmission geometry with the samples introduced in glass capillaries of 0.5 millimetres of diameter, using an incident beam elliptic focalizing mirror and a PIXcel detector with an active detection length of 3.347º. The analysed samples were scanned from 2 to 60º in 2θ, with a step size of 0.026º and a total measuring time of 30 minutes. The routine samples were analysed in a configuration of convergent beam with a focalizing mirror and a transmission geometry with flat samples sandwiched between low absorbing films of polyester of 3.6 microns of thickness, from 2 to 40º in 2θ with a step size of 0.026º and a measuring time of 76 seconds per step. The temperature dependent X-ray powder diffraction experiment was performed in the same experimental device with an Oxford Cryosystems 700 Series Cryostream Cooler temperature system installed.

3. Single crystal X-ray diffraction

MAR345 diffractometer with an image plate detector has been used. Intensities have been collected with graphite monochromatized MoK_{α} radiation using ϕ-scan technique. Reflections were assumed as observed applying the condition $I > 2\sigma(I)$. The structures were solved by Direct methods, using SHELXS computer program (Sheldrick, G.M., 1997)[11] and refined by full-matrix least-squares method with SHELX97 computer program (Sheldrick, G.M., 1997).[11] The function minimized was Σ w $\left| \left| Fo \right|^2 - \left| Fc \right|^2 \right|^2$, where w = $[\sigma2(I) + (0.0575P)^2]^{-1}$ (Form I) and w = $[\sigma2(I) + (0.0409P)^2 + 4.6055P)^2]^{-1}$ (Form II), P = $(\left| Fo \right|^2 + 2 \left| Fc \right|^2)/3$, f, f' and f'' were taken from International Tables of X-Ray Crystallography.[12] All H atoms were computed and refined, using a riding model with an isotropic temperature factor equal to 1.2 time the equivalent temperature factor of the atom which are linked. Number of refined parameters was 208. Max. shift/esd = 0.00, Mean shift/esd = 0.00. Supplementary crystallographic data for Form I[13] and Form II[14] are included in CIF files.

4. Differential scanning calorimetry (DSC)

Differential scanning calorimetry was carried out by means of a Mettler-Toledo DSC-822e calorimeter. Experimental conditions: aluminum crucibles of 40 µL volume, atmosphere of dry nitrogen with 50 mL/min flow rate, heating rate of 10ºC/min. The calorimeter was calibrated with indium of 99.99% purity.

5. Thermogravimetric analysis (TGA)

Thermogravimetric analyses were performed on a Mettler-Toledo TGA-851e thermobalance. Experimental conditions: alumina crucibles of 70 µL volume, atmosphere of dry nitrogen with 50 mL/min flow rate, heating rate of 10ºC/min.

6. Hot-Stage Microscopy (HSM)

A Nikon polarization microscope (Nikon Eclipse 50i) equipped with a Linkam LTS350 hot stage and digital video recorder facilities was used.

7. Theoretical calculations

All single point and geometry optimization have been performed at the M06-2X[15]/6-311+G(d)[16] level followed by an energy evaluation at the MP2[17]/6-311+G(d)[16] level. This computational level has been selected since MP2 is known to give accurate estimates of the interaction energy in intermolecular interactions where dispersion can be relevant, as in the present case, providing accurate quantifications at a reasonable computational cost.[18] All calculations have been carried out using the Gaussian09 package.[19] In all interaction energies, the Basis Set Superposition Error (BSSE) has been corrected using the counterpoise method.[20]

RESULTS AND DISCUSSION

1. Crystal structures of two experimental polymorphs of 1

After the above mentioned polymorph screening (using different combinations of solvents in both thermodynamic and kinetic conditions) only two anhydrous forms of **1** were found, hereafter named Form I and Form II, respectively, whose crystal structures were solved by single crystal X-ray diffraction at 293 K (Table 1).

Table 1 Crystallographic data for the two polymorphs of **1**

Crystal data	Form I	Form II
Empirical formula	$C_{18}H_{14}NO_3P$	$C_{18}H_{14}NO_3P$
Formula weight	323.27	323.27
Temperature	293 K	293 K
Crystal system	Monoclinic	Monoclinic
Space group	$P2_1/c$	C2/c
Unit cell dimensions	$a = 10.075(6)$ Å	$a = 18.635(9)$ Å
	$b = 11.026(6)$ Å	$b = 10.871(4)$ Å
	$c = 16.317(8)$ Å	$c = 16.459(5)$ Å
	$\beta = 119.16(3)°$	$\beta = 107.05(2)°$
Volume	1582.9(15) Å^3	3188(2) Å^3

Z	4	8
Density	1.357 Mg/m^3	1.347 Mg/m^3
Absorption coefficient	0.188 mm^{-1}	0.186 mm^{-1}
F(000)	672	1344
Reflections collected	14640	12357
Independent reflections	5002	4195
R(int)	0.0592	0.0489
Goodness-of-fit on F^2	1.073	1.205
Final R indices [I>2σ(I)]	R1=0.0522,	R1=0.0793,
R indices (all data)	wR2=0.1189	wR2=0.1557
	R1=0.0927,	R1=0.0958,
	wR2=0.1338	wR2=0.1669
Largest diff. peak and hole	0.164 and -0.243 eÅ^{-3}	0.307 and -0.390 eÅ^{-3}
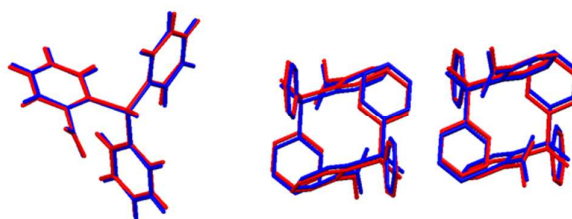
Fig. 2 Overlay of the molecules in Form I (blue) and II (red).

Form I crystallises in the monoclinic space group P21/c with four molecules in the unit cell, whereas Form II crystallises in the monoclinic space group C2/c with eight molecules in the unit cell. Both polymorphs present a 50:50 racemic mixture of *Ps* and *Ms* enantiomers (their crystal space groups P21/c and C2/c respectively contain an inversion centre) with virtually the same intramolecular geometry for **1**. Table 2 collects, for both polymorphs, the most relevant structural parameters defining the intramolecular structure of the molecules of **1**: the three P-C bond lengths, the P-O length, the C-P-O angles, the torsion angles and the shortest PO···O$_2$N distance. As observed in Table 2, there are little variations of these structural parameters between the two forms.

Table 2. Relevant structural parameters for both forms of **1**

Distances and angles	Form I	Form II
Bond distance P-O1 (Å)	1.485(1)	1.481(2)
Bond distances P-C1 (Å)	1.821(2)	1.828(3)
Bond distances P-C7 (Å)	1.804(2)	1.804(3)
Bond distances P-C13 (Å)	1.797(2)	1.802(3)
Bond angles C1-P-O1	111.71(8)°	112.09(13)°
Bond angles C7-P-O1	111.45(9)°	111.93(12)°
Bond angles C13-P-O1	113.66(8)°	113.69(13)°
Torsion angle O1-P-C1-C2	34.9(2)°	37.6(3)°
Torsion angle O1-P-C7-C8	50.1(2)°	46.8(2)°
Torsion angle O1-P-C13-C14	21.2(2)°	25.4(3)°
Distances PO1···O3, (Å)	2.971(3)	2.983(3)
Distance PO1···N1 (Å)	2.940(3)	2.988(3)

As both polymorphs show virtually the same conformation, the only significant structural differences can be found in the molecular packing arrangement. The two polymorphic forms exhibit a very close structural relationship, based on a common 2D packing fragment (Fig. 2). Layers incorporating groups of two molecules of **1** are stacked in the same fashion in both polymorphs. However, the neighbouring layer is translated along the respective *c*-axis in one

polymorph respect the other one (see Figure 3, note at the direction of the PO group inwards or outwards). The following layers are again equal in both forms and so on. Forms I and II may therefore be interpreted as two distinct packing modes of the common 2D unit. The presence of two or more alternative stacking modes of a common 2D structure fragment is probably one of the most important kinds of polymorphism which can be observed in molecular crystal structures.[21]
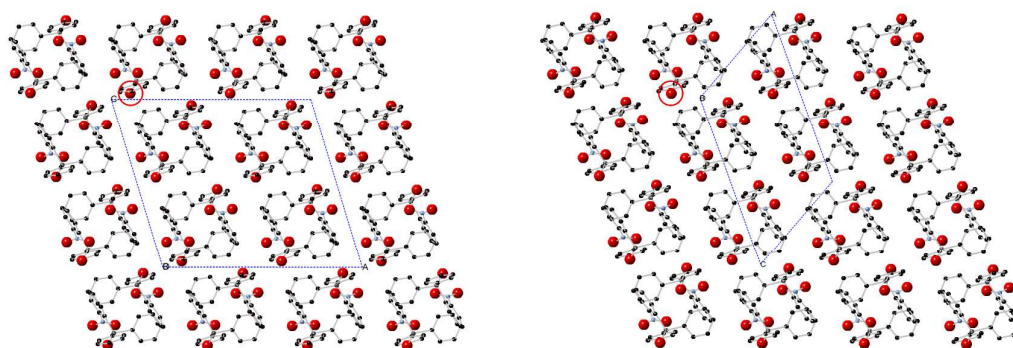
Fig. 3 2D packing similarity of forms I (left) and II (right). Note the difference in the direction of the PO group inwards or outwards.

Weak hydrogen bonds of the type CH···OP can be identified in each layer and between layers of both polymorphs, involving the oxygen of the phosphine oxide group and an aromatic hydrogen. Moreover, CH···π interactions (distance to the centroid: 3.17 and 3.01, distance to the plane: 2.84 and 2.75, H: 1.41 and 1.22 and α: 156 and 160º respectively in forms I and II) involving the nitrophenyl of one molecule and a phenyl of an adjacent molecule are observed also in each layer of both forms. Additional π-π interactions are found between layers only in Form II, involving the nitrophenyl groups of different molecules. The observed lateral offset stack is 1.40 Å,[22] the centroid to centroid distance, d(π···π), is 3.98 Å, the interplanar distance 3.72 Å and the dihedral angle α is 34º.

Finally, it is worth mentioning some aspect of the nitro groups geometry in Form I and II. The nitro group in other crystal structures, such as these of nitrobenzene, 1,3- and 1-4-dinitrobenzenes, tends to be coplanar with the aromatic ring, due to conjugation with their π-systems. However, in 1,2-dinitrobenzene the nitro groups shows a notable torsion angle between the aryl and the NO_2 planes (of -51.05º if Form I and 51.95º in Form II), large values of such rotation angle result in reducing the π-conjugation with the aromatic system.[23] Thus, the rotation observed in the molecules of **1** suggests a repulsive nature for these PO···O_2N interactions in the *syn* conformation of **1**, which wouldn't exist if the nitro group were located *anti* to the PO, although intra- and intermolecular CH···O interactions may also contribute. However, in both polymorphs of **1** the nitro group shows a *syn* relationship to the PO, thus allowing the formation of short intramolecular PO···O_2N contacts: 2.971(3) in Form I and 2.983(3) in Form II, both shorter than 3.04 Å, the sum of the two oxygen Van der Waals radius (1.52 Å). Such a short distances are usually indicative of the attractive nature of the corresponding interactions. The resolution of this puzzle is possible by doing accurate computational studies on the proper model systems (see below).

2. Hirshfeld surface analysis

Since no substantial conformational differences are observed, the Hirshfeld surface analysis seemed to be a particularly promising tool to in the visualisation of variations in the intermolecular geometries of both polymorphs of **1**. The Crystal Explorer[24] program was used for such analysis. The resulting 2D fingerprint plots are given in Figure 4

where it is easy to recognize qualitatively the differences in the environment of the molecules, despite the apparent similarity in their 2-dimensional packing arrangement. The CH···π interactions (marked with **a** in Fig. 4) are observed as wings at $d_e \approx d_i$ at around 1.6 Å in both polymorphs. The weak hydrogen bonds CH···OP (marked with **b** in Fig. 4) are observed as two spikes at $d_e \approx d_i$ at around 1.3 Å in Form I and 1.4 Å in Form II. These interactions are not apparent in the fingerprint when they are superimposed on the sharp spikes of other strong hydrogen bonds. H···H interactions (marked with **c** in Fig. 4) appear at $d_e \approx d_i$ at around 1.3 Å in Form I and 1.15 Å in Form II. The π-π stacking (marked with **d** in Fig. 4) appears as a pale blue-green colour on the diagonal of the fingerprint plot with $d_e \approx d_i$ at around 1.75 Å, only in Form II.
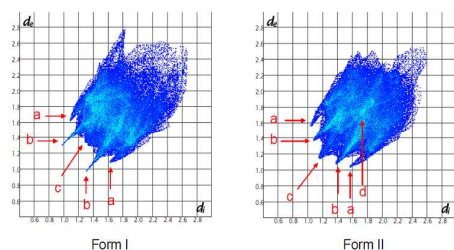
Fig. 4 2D fingerprint plots for Form I and II; d_e and d_i are the distances to the nearest atom centre exterior and interior to the surface.

3. Thermal analysis and thermodynamic stability

The two polymorphs of **1** show a similar melting temperature. As shown in the DSC in Figure 5, after the melting of Form I at 221ºC, Form II crystallises from its melt (confirmed by thermomicroscopy (Fig. 6) and temperature variable PXRD (Fig. 7). On the other hand, Form II shows a unique melting endotherm at 224ºC.
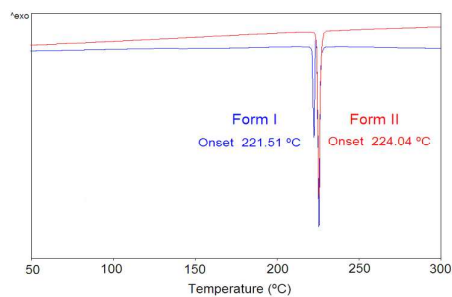
Fig. 5 DSC of Form I and Form II of **1**.
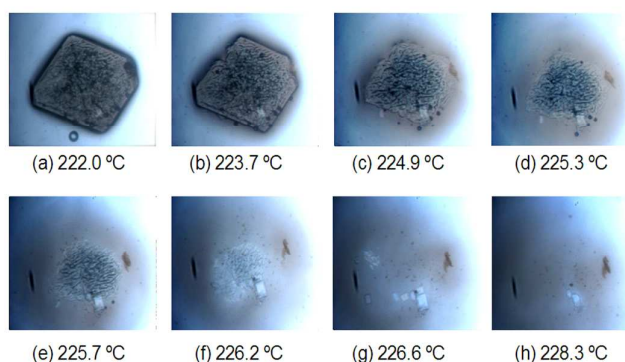
Fig. 6 Hot stage photomicrographs in polarized light, showing the melting of Form I (c) followed by crystallization of Form II (d) which finally melts (h).

In order to study their relative thermodynamic stability, a solution mediated transformation experiment was carried out in ACN with a mixture of both forms. After 3 days at r.t., the mixture transformed into Form I, revealing that Form I is the most stable polymorph at this temperature. This result agrees well with the order of density values (I: 1.357 > II: 1.347) obtained from the crystal structures. It is worth remarking that, once again, all molecules of **1** are in their *syn* conformation.
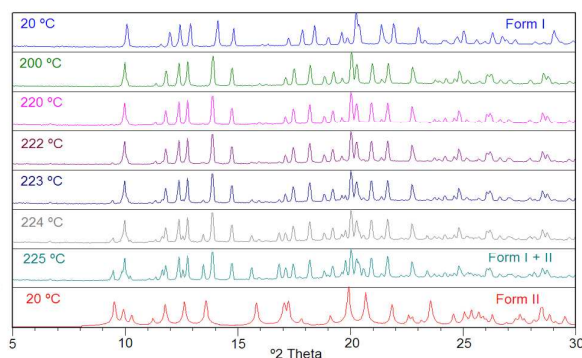
Fig. 7 Temperature variable PXRD showing the transformation of Form I into a mixture of forms I and II at 225ºC. At the bottom, PXRD pattern of Form II calculated from single crystal data.

4. Computational results

The following three major issues remain un-answered after the previous experimental studies: (i) What is the nature of the interaction between the PO and NO_2 groups?, (ii) Why the two polymorphs of **1** (Forms I and II) show the same geometry (in the racemic mixture of *Ps* and *Ms* enantiomers)?, and (iii) Why the *Pa* and *Ma* isomers are not observed?. In order to clarify these issues, an exhaustive energetic and structural analysis of **1** has been carried out based on the results of MP2 *ab initio* calculations.

a. The nature of the PO···O2N intramolecular interaction

We first address the presence of an intramolecular interaction between the NO_2 and PO moieties by using a simple model system consisting of one H_3PO and one NO_2H molecules, aimed a mimicking the PO and NO_2 groups in the crystal. It is worth mentioning that this model allows to study the interaction of interest, while also minimizes all other possible secondary inter-molecular interactions (for instance, if H atoms were substituted by methyl groups in Fig 8a, CH···O interaction would be also present). Two different arrangements of the model system were studied, differing in the pathways along which the two fragments approach (Fig. 8).
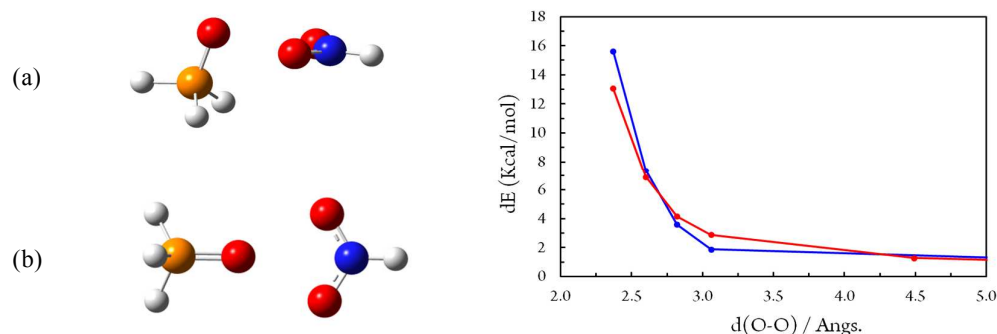
Fig. 8 Scheme of the model system employed in the evaluation of the *PO···O$_2$N* intramolecular interaction. The energy evolution of the (a, blue) lateral and (b, red) confronted approaches has been explored. Energy axis is referred to the energy of the isolated constituents.

The two scenarios indicate an increase in the total energy of the complex as the molecules approach, a fingerprint of a repulsive interaction. In the two polymorphs of **1**, the closest PO···O$_2$N distance is 2.971(3) Å (Form I) or 2.983(3) Å (Form II), at this distance (~ 3 Å), the two models (A and B) yield an interaction energy of 1.9 and 2.9 Kcal/mol, respectively. However, it should be noted that in the two models, the three oxygen atoms have been symmetrically confronted, while in the crystal structure its inter-atomic distance is asymmetric (2.9 Å and 3.5 Å). Furthermore, the N atom has been set collinear to the (P)O···O(N) interaction, resulting in a larger PO···NO$_2$ at any given PO···O$_2$N distance, while in the crystal structure both distances are similar (see Table 2). In view of the potential contribution of the selected dispositions in the calculated interaction energies, we have positioned our model system in the same arrangement as in **1** (Fig. 9) and calculated the intermolecular interaction at this orientation (as: $E_{int} = E_{Tot} - E_{H3PO} - E_{NO2H}$). A repulsive intermolecular interaction of 4.8 kcal/mol was obtained. Note that this value must also be taken with caution as it presents a potentially attractive H···H interaction, not found in **1**.
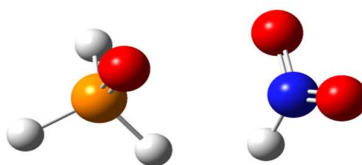
Fig. 9 Scheme of the model system employed in the evaluation of the *PO···O$_2$N* intramolecular interaction when the PO and NO_2 groups are positioned as in the crystal structure of **1**.

Overall, our results on the model systems confirm that the PO···O_2N intramolecular interaction is of repulsive nature, with a strength that may be found around 4.8 kcal/mol at the crystal geometry, according to our MP2 calculations. These results were expected since atoms with net negative charge are confronted. However, the exclusive presence of *syn* conformers in the crystal structure of **1** prompted us to analyse the nature of this interaction in more detail.

b. Conformational analysis.

The relative stability of the *anti* and *syn* conformations of the NO_2 group in **1** (hereafter called **1-anti** and **1-syn** respectively) has been first addressed by comparing its minimum energy structures (Fig. 10). Our results show that **1-anti** is *ca.* 1 Kcal/mol more stable than **1-syn**. This is in contrast to the exclusive presence of the *syn* conformation on the crystal structure of **1**. The origin of the increased stability of the *anti* conformation can now be confidently attributed to the presence of a repulsive interaction between the NO_2 and PO groups in **1-syn** and absent in **1-anti**, favouring the stability of the latter. It is also worth pointing out that in both optimum geometries the NO_2 group is non-coplanar with the aryl group to which it is attached.
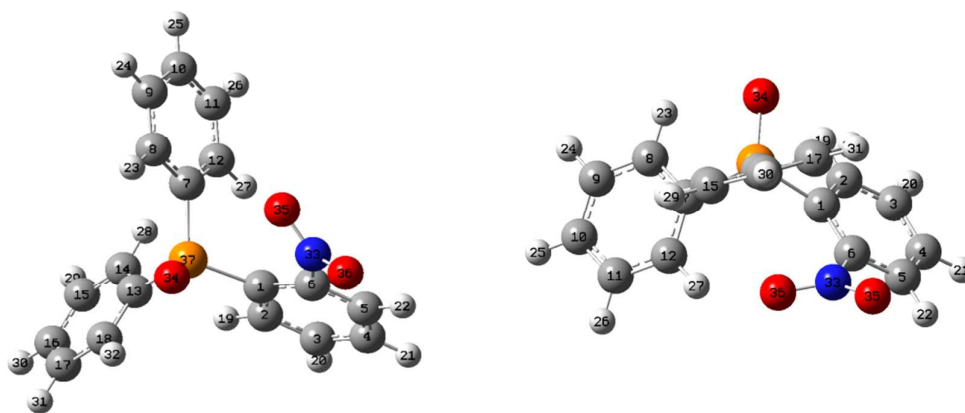
Fig. 10 Optimized structures of (left) **1-syn** and (right) **1-anti** conformations of **1**. Atom labels are shown. Color code: C (gray), H (white), O (red), N (blue), P (orange).

In order to explain the conformational preferences of **1** on solid energetic considerations, the potential energy surface along the **1-syn** → **1-anti** rotation was computed and analyzed. The energies corresponding to torsion angles involving atoms 34-37-1-6 (see Figure 10) was calculated at values that range from -165º to +165º (such angle is -34.9(2)º in Form I and 37.6(3)º in Form II, Fig. 11). All other variables were allowed to optimize. The results, presented in Figure 11, show that the energetic profile of the rotation is symmetric and centered at 0º (where the maximum overlap between NO_2 and PO units is produced). **1-anti**, (corresponding to torsion angles close to 180º, is about 1 kcal/mol more stable than **1-syn**. Two local minima exist at around +35º and -35º, corresponding to the two symmetric *syn* conformations (*Ps* and *Ms*) that may easily interconvert through the (*Ps* → *anti* → *Ms*) path, surpassing two small barriers of *ca.* 1 kcal/mol. In contrast, the repulsive interaction between the NO_2 and PO units creates a barrier of *ca.* 3.8 kcal/mol along the 'shorter' (*Ps* → 0º → *Ms*) path.
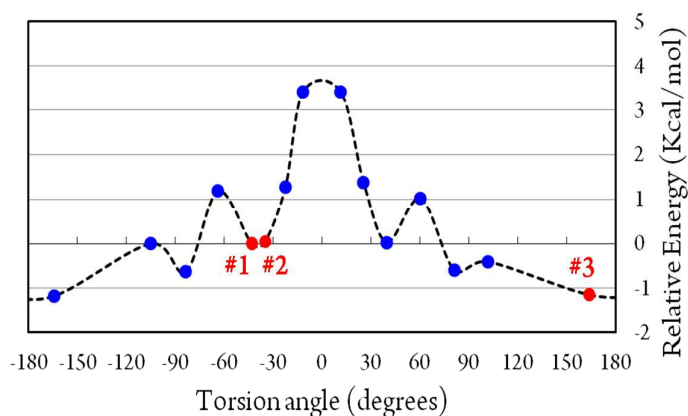
Fig. 11 Energy evolution along the *syn* → *anti* coordinate. Three points have been highlighted in red: #1: Minimum energy structure for the *syn* conformation. #2: Crystal structure. #3: Minimum energy structure for the *anti* conformation. Energy reference has been set at the value of #1.

In summary, our isolated molecule calculations on **1** suggest that **1-*anti*** is slightly more stable than **1-*syn***, the conformation observed in the crystal structure of **1**, and that these two conformations may easily interconvert at room temperature, due to the presence of small interconversion barriers. These results suggest that, based on energy criteria, the enantiomers *Pa* and *Ma* might also be found in the crystals of **1**.

c. Crystal packing analysis

As shown in the preceding sections, the reason behind the observation of, exclusively, *syn* conformers in the crystal structure of **1**, has not been identified at the molecular level. Therefore, our next step is to analyze whether the energetic factors control the crystal packing of the material.[25] For the sake of simplicity, we have adopted Form I (which is the most stable at r.t.) as representative. We have quantified the intermolecular interactions between all the symmetry-unique dimers[26] (*d1-d6*) present on it (each dimer is constituted by two molecules of **1**, see Figure 12 for crystal topology and Figure 13 for crystal pairs). The results of these computations cannot be directly compared against those found in dimers whose molecules are in an *anti* conformation, because the crystal structures of such polymorphs (*Pa* and *Ma*) are not known. Two factors restrained us from doing a polymorph prediction of the molecules of **1** in their *anti* conformation. Most of those codes are based on propagating the optimum geometry of the structure-directing pairs (that is, those pairs having interaction energies notably more stable than the others) along the symmetry elements of the crystal. However, our results indicate that: (a) in Form I, all dimers have similar interaction energies (see Table 3), and (b) during the geometry optimization of the *syn* **1···1** pairs, they undergo an important geometrical relaxation from their initial structure (the experimental crystal structure). Such relaxation is at odds with the essence of these prediction algorithms, which assume that the crystal structure of the pairs is close to a minimum energy structure of the pair.
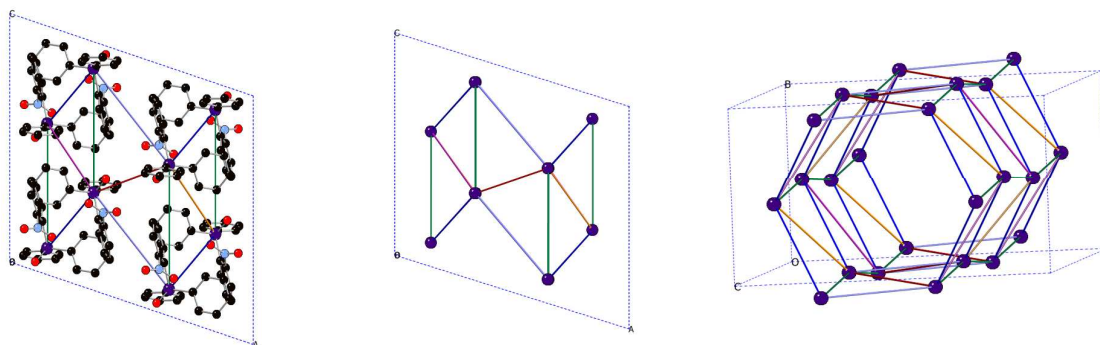
Fig. 12 Crystal structure views of Form I: (left) along the a-c plane, (center) schematic representation of the **1-1** pairs along the same view, where only the P atoms are shown, and (right) three-dimensional view showing all the **1-1** pairs. Red, blue, green, orange, magenta and pale-blue lines represent dimers *d1-d6*, respectively.

In order to have dimer structures in which a direct comparison of interaction energies is possible, we have optimized the geometry of the (*d1-d6*) dimers when its constituents are found either in *syn* or in *anti* conformations, obtaining the hereafter called opt-*syn* and opt-*anti* pairs. When searching for opt-*syn* pairs, the initial pair structure in the optimization procedure is exactly that of the crystal geometry. Similarly, for the opt-*anti* pairs, the initial pair structure has been generated by rotation of the substituted benzene group from its disposition on the crystal structure. At the end of the optimization procedure, the resulting opt-*syn* pairs present the same relative orientation as in the crystal structure, while some changes are observed for opt-*anti*, in accordance with the changes undergone by its monomers (see Figure 13 for resulting structures and Table 3 for energetic results).

Table 3. Interaction energies and monomer-monomer distances of the simmetry-unique pairs found in **1** at its crystal structure and in the optimized structures for the *syn* (opt-*syn*) or *anti* (opt-*anti*) disposition of its conforming monomers. Note that each monomer has two equivalent *d2* and *d3* dimers on the crystal structure (see Fig 12).

	Crystal structure		opt-*syn*		opt-*anti*	
	d(P-P)	E_{int}	d(P-P)	E_{int}	d(P-P)	E_{int}
d1	5.884	-8.83	5.727	-14.45	5.753	-9.20
d2(2x)	7.367	-7.89	6.917	-12.39	5.818	-15.44
d3(2x)	8.269	-5.22	6.160	-14.97	5.694	-14.84
d4	7.341	-7.48	6.975	-13.11	6.986	-10.27
d5	8.446	-3.46	7.709	-11.09	5.564	-11.44
d6	8.441	-7.02	8.441	-15.26	7.595	-12.82
$\sum E_{int}$		-53.03		-108.63		-104.30

Crystal structure	opt-*syn*	opt-*anti*

d1   -8.83   -14.45   -9.20

d2   -7.89   -12.39   -15.44
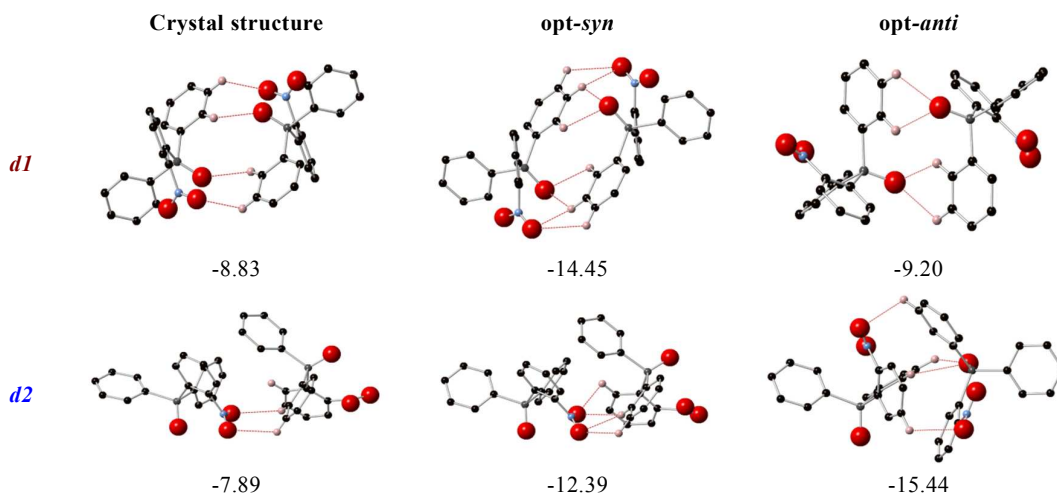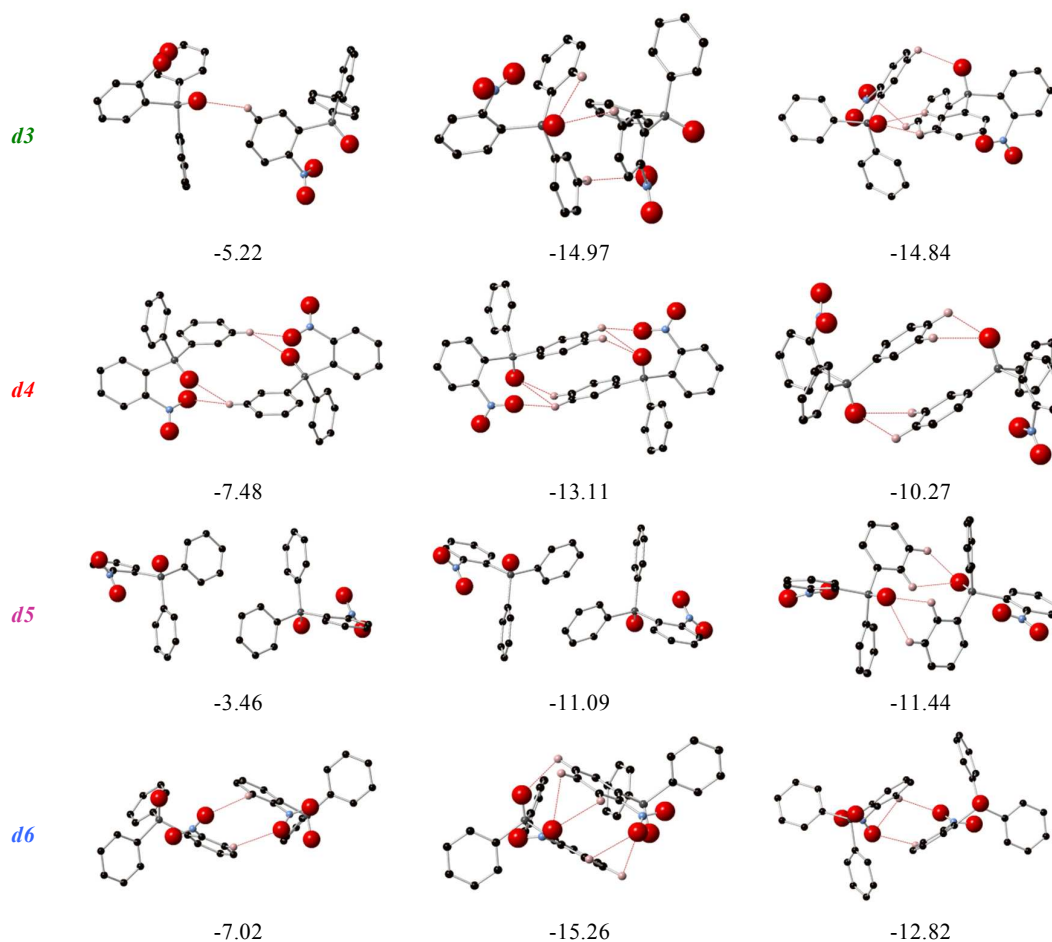
Fig. 13 Interaction energy and geometries for the *d1-d6* dimers in (left) crystal structure and after optimization procedure in (middle) *syn* and (right) *anti* conformations. The potential O···H intermolecular contacts that may stabilize the formation of the pairs has been highlighted. All remaining H atoms have been removed.

In general, each pair tends to maximize the formation of its hydrogen bonds (C-H···O-N, C-H···O-P and C-H···π) to increase their stability. For instance, Table 4 summarizes the structural changes observed for the main intermolecular contacts of *d1* upon the optimization procedures, together with its interaction energy for each structure. Note that in opt-*syn*, there is a shortening of all the intermolecular contacts with respect to the crystal structure, resulting in a notable enhancement of the interaction energy (-8.83 vs. -14.45 kcal/mol). On the other hand, in the opt-*anti* structure, the change on the conformation of each monomer results in two additional PO···H weak bonds while prevents the formation of the two NO···H hydrogen bonds, resulting in a slight increase in interaction energy (-8.83 vs. -9.20 kcal/mol). Among the six pairs studied (*d1-d6*), the stability of *d1* is the most affected by a conformational change from *syn* to *anti*. Finally, we note that the geometry of the molecules in the optimized pairs satisfies the trends drawn in precedent sections when looking at the crystal geometries, namely: (i) No alignment of the NO_2···PO moieties is observed, which is in agreement with such interaction being of repulsive nature; (ii) The O-P-C-C(NO_2) torsion angle in the monomers that form the opt-*syn* pairs are found to be between 32º and 45º, in agreement with this region being a local minimum for the *syn* arrangement, as shown in Figure 11; and (iii) similarly, the monomers that form the opt-*anti* pairs have a O-P-C-C(NO_2) torsion angle between 159º and 176º, in agreement with this region being a local minima for the *anti* arrangement, Figure 11.

Table 4. Comparison of the intermolecular contacts and interaction energies in dimer 1. All distances are given in Angstrom and interaction energy is given in Kcal/mol

	Crystal structure	opt-*syn*	opt-*anti*
Distance (P-P)	5.88	5.73	5.75
Distance (PO⋯H)	2x (2.56, 3.15)	2x (2.33, 2.60)	2.27, 2.61, 2.43, 2.50
Distance (NO⋯H)	2x (2.85, 3.81)	2x (2.60, 2.80)	-
E_{int}	**-8.83**	**-14.45**	**-9.20**

The differences observed in the interaction energies of the pairs when the structure is optimized can be rationalized in the following way: while the molecules in the crystal adopt a disposition that maximizes their contacts with all its neighbours at a time, in opt-*syn* and opt-*anti*, they seek to maximize the intermolecular contacts with the given pair of molecules (*d1-d6*), separately, thus increasing the pair interaction energies with respect to that in its original crystal structure. The situation has some resemblance to that encountered during the nucleation stage of a crystallization process, where all molecules seek to maximize their intermolecular interaction energy with all their neighbours (that is, lower the free energy of the aggregate), without the symmetry constraints imposed by the crystal. The small difference found between the sum of the intermolecular interaction energy of the *syn* and *anti* conformations (-108.63 vs. -104.30 kcal/mol, Table 3) indicates that the pairs are able to make more attractive interactions when all molecules adopt a *syn* conformation. This could be a reason in favour of the presence of the *syn* conformation despite the repulsive character of the PO⋯O_2N interaction. Note, however, that the selection of the symmetry-unique dimers is based on the crystal structure of **1**, which may be biasing our results towards a favoured *syn* arrangement. A definitive conclusion cannot be reached without an experimental crystal structure for the *anti* conformation.

A proper rationalization of the causes of the energetic gains observed upon the geometry optimization of the molecular pairs can only be done in terms of the intermolecular interaction present within these pairs, looking at the changes during the optimization of the geometrical parameters that characterize the interaction energy of these interactions (see Table 4).[27] The power of the intramolecular bond concept in chemistry rests in that it allows good approximations to the energetic change caused by geometrical, that is, of the internal energy as a sum of bond energies. Supramolecular interactions are weaker and, consequently, prone to change with temperature or other external perturbation. But, even so, supramolecular interactions are still the only simple tool which allows to connect geometry with energy. Thus, using supramolecular interaction it is possible to explain why some pair-geometries are energetically more stable than others.

CONCLUSIONS

Two polymorphs of *o*-nitrophenyldiphenylphosphine oxide **1** have been found after a polymorph screening, both showing the same *syn* conformation of the NO_2 group with respect to the PO moiety, where short PO⋯O_2N contacts are formed. However, MP2 calculations have shown the repulsive nature of this PO⋯O_2N intramolecular interaction. Despite the apparent similarity in the 2D packing arrangement of both forms, the Hirshfeld analysis has allowed to recognize the differences in the environment of the molecules of both polymorphs, i.e. the presence of a π-π stacking only in form II.

We have calculated the energetic profile of the rotation that connects the *Ps* and *Ms* enantiomers through the two possible pathways (*Ps* → *anti* → *Ms* and *Ps* → Torsion Angle = 0° → *Ms*). By doing this, we have shown that these two conformations may easily interconvert at room temperature due to the absence of significant barriers of rotation.

The energetics of one of the polymorphs (Form I) was analyzed by calculating the interaction energy of each

symmetry-unique **1-1** pairs (*d1-d6*) found on it. In view of the results we have concluded the (a) absence of structure-directing pairs and (b) the slightly larger attractive interactions between pairs when each constituent adopts the **1-*syn*** conformation. This would be a possible way of explaining the adoption of this disposition despite the repulsive PO···O_2N interaction. However, since both *syn* and *anti* conformers are close in energy, both in the gas phase and in the crystal packing, there are no possible thermodynamic factors explaining the absence of the *anti* conformation. Therefore, we hypothesize that the only reasons for such an absence has to be on the kinetic factors that influence the nucleation process, and thus control the final outcome of the crystallization. Unfortunately, due to the lack of a crystal structure for the *anti* conformation of **1**, the reason behind the observation of, exclusively, *syn* conformers in the crystal structure of **1**, has not been found.

ACKNOWLEDGEMENTS

ELECTRONIC SUPPLEMENTARY INFORMATION AVAILABLE (ESI)

Ortep representations of Form I and Form of *o*-nitrophenyldiphenylphosphine oxide (**1**) are available.

REFERENCES

[1] A. Pintér, G. Haberhauer, I. Hyla-Kryspin and S. Grimme, *Chem. Commun.*, 2007, 3711-3713.

[2] R. K. Palmer, R. Bryant and D. Sprous, Triphenylphosphine oxide derivatives and uses thereof, 2008, WO2008033545A2.

[3] M. C. Etter, P. W. Baures, *J. Am. Chem. Soc.,* 1988, **110**, 639-640.

[4] S. Brydges and M. J. McGlinchey, *J. Org. Chem.*, 2002, **67**, 7688-7698.

[5] T. Benincori, A. Marchesi, P. R. Mussini, T. Pilati, A. Ponti, S. Rizzo and F. Sannicolò, *Chem. Eur. J.*, 2009, **15**, 86-93. Alternative descriptors for propellers have been suggested, which, however, require the introduction of symbols not familiar to the stereochemical language.

[6] B. Laleu, G. Bernardinelli, R. Chauvin and J. Lacour, *J. Org. Chem.*, 2006, **71**, 7412-7416.

[7] G. Haberhauer, S. Ernst and C. Wilch, *Chem. Eur. J.*, 2011, **17**, 8643-8647.

[8] D. Gust and K. Mislow, *J. Am. Chem. Soc.*, 1973, **95**, 1535-1547.

[9] P. Calcagno, B. M. Kariuki, S. J. Kitchin, J. M. A. Robinson, D. Philp and K. D. M. Harris, *Chem. Eur. J.*, 2000, **6**, 2338-2349.

[10] J. I. G. Cadogan, D. J. Sears and D. M. Smith, *J. Chem. Soc. (C)*, 1969**,** 1314-1318.

[11] G. M. Sheldrick, *Acta Crystallogr.*, 2008, **A64**, 112.

[12] *International Tables of X-Ray Crystallography*, Kynoch press, 1974, **Vol. IV**, pp 99-100 and 149.

[13] CCDC 990187 contains the supplementary crystallographic data for Form I.

[14] CCDC 990188 contains the supplementary crystallographic data for Form II.

[15] Y. Zhao and D. G. J. Truhlar, *J. Chem. Phys.*, 2006, **125**, 194101.

[16] (a) A. D. McLean and G. S. Chandler, *J. Chem. Phys.*, 1980, **72**, 5639-5648 (b) K. Raghavachari, J. S. Binkley, R. Seeger and J. A. Pople, *J. Chem. Phys.*, 1980, **72**, 650-654.

[17] C. Møller and M. S. Plesset, *Phys. Rev.*, 1934, **46**, 618-622.

[18] K. E. Riley, J. A. Platts, J. Řezáč, P. Hobza and J. G. Hill, *The Journal of Physical Chemistry A,* 2012, **116**, 4159.

[19] M. J. Frisch et al., *Gaussian 09, Revision B.01*, Gaussian, Inc: Wallingford, CT., 2009.

[20] S. F. Boys and F. Bernardi, Mol. Phys., 1970, **19**, 553–566.

[21] D. E. Braun, T. Gelbrich, V. Kahlenberg, G. Laus, J. Wieser and U. J. Griesser, *New. J. Chem.*, 2008, **32**, 1677-1685.

[22] C. A. Hunter and J. K. M. Sanders, *J. Am. Chem. Soc.*, 1990, **112**, 5525-5534.

[23] I. V. Omelchenko, O. V. Shishkin, L. Gorb, F. C. Hill and J. Leszczynski, *Struct. Chem.*, 2012, **23**, 1585-1597.

[24] J. J. McKinnon, M. A. Spackman and A. S. Mitchell, *Acta Cryst*, 2004. **B60**, 627. Illustrations with computer package *CrystalExplorer v2.1*: S. K. Wolff, D. J. Grimwood, J. J. McKinnon, D. Jayatilaka and M. A. Spackman. University of Western Australia, Perth, Australia, 2007.

[25] We understand as energetic factors (also called thermodynamic) those affecting the relative stability of the minimum energy structures, while kinetic factors are those affecting the energy barriers connecting those minima.

[26] Defined as all pairs generated from the unit cell, which are not related among themselves by any of the symmetry operations present in the crystal.

[27] Gavezzotti, A. CrystEngComm 2013, **15**, 4027

TOC (text and figure)

An experimental and computational study of the polymorphism of o-nitrophenyldiphenylphosphine oxide (**1**) has been carried out raising the question of why the *anti* polymorphs, more stable than the observed *syn* conformations, according to our computations, have not been found.